Copy Move Image Forgery Detection Method Using Steerable Pyramid Transform and Texture Descriptor

Ghulam Muhammad[1], Muneer H. Al-Hammadi[1], Muhammad Hussain[2], Anwar M. Mirza[1], and George Bebis[3]

[1]*Dept. of Computer Engineering,* [2]*Dept. of Computer Science,*

College of Computer and Information Sciences, King Saud University, Riyadh, Saudi Arabia

Email: {ghulam, mhussain, ammirza}@ksu.edu.sa, eng.muneer2008@gmail.com

[3]*Dept of Computer Science and Engineering, University of Nevada at Reno, USA*

Email: bebis@cse.unr.edu

Abstract— **In this paper, we propose a passive copy move image forgery detection method using a steerable pyramid transform (SPT) and Local Binary Pattern (LBP). SPT is applied on a grayscale version or one of the YCbCr channels of an image. LBP is applied to describe the texture in each SPT subband. Then the support vector machine (SVM) uses the LBP feature extracted from SPT sub-bands in classifying images into tampered or authentic images. Experimental results show an excellent effectiveness for the proposed method in some combinations of SPT sub-band.**

Keywords: luminance, chrominance, Steerable pyramid transform, local binary pattern, copy move image forgery, support vector machine

I. INTRODUCTION

Images are one of the natural carriers of information. Currently, they are the most common and convenient way for expressing and transmitting information. Information expressed in thousands of words can be easily and compactly expressed in a simple image. The human being a visual system has a high ability in deriving pictorial information extremely faster than any other kind of information. Pictorial information represents nearly 75% of all the information received by human visual system [1]. Digital images play a very important role in our community in a wide variety of applications. They are everywhere in our life, for example, in military applications, in insurance processing, in surveillance systems, in intelligence services, in medical imaging, in the internet websites, on the TV and advertisement media, on the cover of magazines and newspapers, in the forensic investigation, etc. [2], [3]. Unfortunately, this high popularity of digital images and the development in image's editing and manipulating computer software that are low-cost, user-friendly and powerful such as Adobe Photoshop, made it easy to edit digital images and led to a rapid increase in digitally tampered images in mainstream media and on the Internet which decreases the credibility of digital images, and their content integrity can no longer be fully trusted [2].

One of the most important and widely used image tampering techniques is copy-move image forgery. The purpose of such tampering is to duplicate or conceal a certain object in an image. Performing of post-processing operations such as blurring, adding noise and JPEG compression or geometric operations such as scaling, shifting and rotation increases the hardness of the detection tasks. Therefore, it is required for any suggested detection algorithm to be robust against such operations [4].

In order to recover people's confidence in the authenticity of digital images, many studies have been done. Fridrich *et al* [5] and Huang [9] used Discrete Cosine Transform (DCT) coefficients as a feature vector to represent an image in their proposed block matching based methods of copy move forgery detection. Popescu *et al* [6] proposed another block matching method where the Principal Component Analysis (PCA) extracted from each individual block in the grayscale version of an image and used to represent the feature vector of that block. For the purpose of dimensionality reduction, feature vectors are truncated and then quantized before being used for block matching detection. Li *et al* [7] proposed a method based on Discrete Wavelet Transform (DWT) and Singular Value Decomposition (SVD). DWT is calculated for the grayscale version of an image, and only the low-frequency component (LL) is used to represent that image. LL is divided into overlapping blocks. Block matching is based on the SVD features extracted from each block. Bayram *et al* [8] suggested using Fourier-Mellin transform as a feature vector for each block after dividing the questioned image into overlapping blocks. They try to find matching between different blocks based on the similarity of different feature vectors. Muhammad *et al* [10] proposed a copy move forgery detection method based on Dyadic Wavelet Transform. They invested two types of information in order to detect a duplication forgery in an image: the similarity between the duplicated regions in the smooth version of the image (approximation sub band LL1) and the dissimilarity caused by noise inconsistency in detail sub band (HH1).

In this paper, we propose a passive copy move forgery detection algorithm based on Steerable Pyramid transform-Local binary Pattern (SPT-LBP). SPT is applied on chrominance component of a color image and LBP features are extracted from the resultant sub-bands. Support vector machine (SVM) is applied to detect forged images.

The rest of this paper is organized as follows. In Section II, we present our proposed algorithm in details. Section III

978-1-4673-2232-4/13/$31.00 ©2013 IEEE

presents and discusses the experimental results, and section IV contains conclusion and future work.

II. Proposed Method

Fig. 1 shows a block diagram of the proposed method.

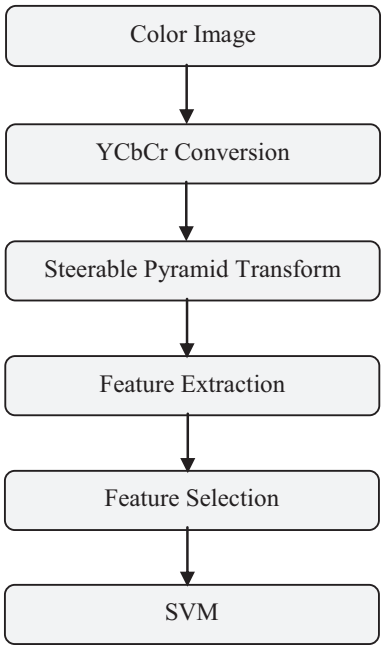

Fig. 1. Steps of the proposed method.

The first step in the proposed method is image preparation. In this step, an input RGB color image is converted into YCbCr chrominance space, where Y is the luminance, and Cb and Cr are the blue difference and the red difference of chrominance components, respectively. From this point on, each of YCbCr channel will fully represent the original color image and will be separately tested. Then a SPT is applied to each component of YCbCr. A 3- level by 4- orientation SPT is used to represent an image by a total number of 12 sub-bands with a wide range of scale and orientation variety, in addition to the lowest frequency sub band.

The second step is feature extraction, where LBP is applied on each individual sub-band of the SPT. The normalized LBP histogram is extracted and used as a feature vector for the corresponding sub-band.

The third step is feature selection. Two different data reduction methods were used for feature selection, Feature Discriminant Ratio (FDR) and LOGO [15]. A cascading of the two methods is also used to enhance the ability of omitting irrelevant features and overcome the complexity of data distribution. Finally, the SVM classification is used to evaluate the performance of the proposed method.

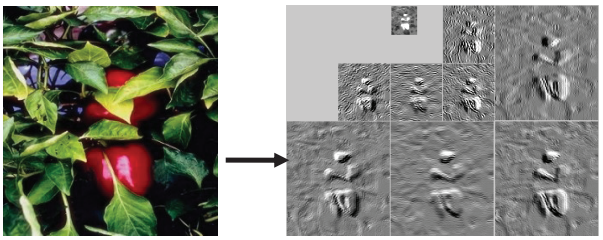

Fig. 2. An example of a 2-level by 4-orientation SPT.

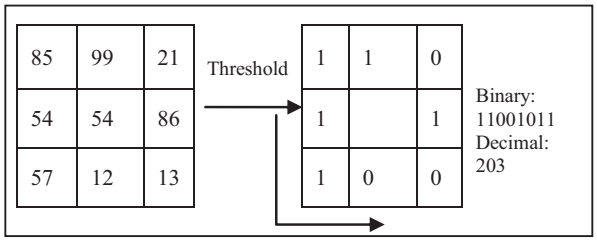

Fig. 3. Basic LBP operator.

A. Steerable Pyramid Transform (SPT)

SPT is a powerful linear multi-scale, multi-orientation image decomposition technique. It was developed to overcome the limitations of orthogonal separable wavelet decompositions. The steerable pyramid analysis functions are dilated and rotated versions of a single directional wavelet [11]. Fig. 2 shows a 2-level by 4-orientation SPT example.

B. Local Binary Pattern (LBP)

LBP is a texture descriptor. It labels each pixel in the image by thresholding the neighborhood pixels with the center pixel value and considering the result as a binary number as in Fig. 3. Then the texture can be described by the histogram of these label values [12]. The operator defines a neighborhood for each pixel as a set of sampling points equally spaced from the pixel to be labeled and located on a circle centered at that pixel.

The extended version of LBP allows any radius for that circle with any number of sampling points. The notation (P, R) is used to mention pixel's neighborhood, where P is the number of sampling points and R is the circle radius. If the sampling point is not exactly in the center of the pixel, it is bilinear interpolated [12]. If the local binary pattern contains at most two translations between 0 and 1, it is called uniform (u2); for example, (11001111) is uniform binary patterns and (11001001) and (01010011) are not. Each uniform pattern is assigned to a separate bin in the histogram while all non-uniform patterns are assigned to a single bin [12].

SPT is used in the proposed method, because the trace of the forgery, which is not visible in a RGB image, can be found in different scales or orientations of that image. Moreover, LBP is a good local texture descriptor and widely used in other image processing applications. While doing forgery, the original texture is distorted, and thereby, the proposed method can encode texture differences at different levels and orientations of a steerable pyramid transformed image.

III. Experimental Results

CASIA TIDE-v1.0 dataset [13] is used in our experiments. The total number of images used is 719, where 260 are authentic images and the remaining 459 copy move forged images. Different post processing operations and geometric translations (such as blurring, scaling and rotation) have been applied on the forged images. All the images have the size 384×256 pixels, and they are in JPEG format. A randomly selected 50% of the whole dataset samples are used for the feature selection step. The LIBSVM toolbox is then used with the reduced dataset for classification. More specifically, RBF (radial basis function) kernel was used in our experiments. The optimal values for the kernel parameters (σ and c) are automatically set by an intensive grid search process using 25% of the whole dataset after reducing the number of features. Moreover, to enhance the SVM classification efficiency a 10 fold cross validation is used. The performance of the proposed algorithm is given in terms of accuracy, sensitivity and specificity as of Eq. (1), Eq. (2), and Eq. (3), respectively.

$$\text{Accuracy} = \frac{TP+TN}{TP+TN+FN+FP}\times 100 \qquad (1)$$

$$\text{Sensitivity} = \frac{TP}{TP+FN}\times 100 \qquad (2)$$

$$\text{Specifity} = \frac{TN}{FP+TN}\times 100 \qquad (3)$$

Where TP (True Positive) is the number of forged images, which are classified as forged images, FN (False Negative) is the number of forged images, which are classified as authentic images, FP (False Positive) is the number of authentic images, which are classified as forged images and TN (True Negative) is the number of authentic images, which are classified as authentic images.

We carried out intensive experiments to test the performance of the proposed method. Many combinations between different image representations (grayscale, Y, Cr and Cb), SPT sub-bands and LBP parameters were used in the evaluation, in order to notice how the performance is affected by different SPT levels, orientations and image components. Different SPT sub-bands combinations are also used to identify the combination that provides the best performance. In case of LBP parameters, we found that zero mapping and u2 mapping performed the best, where u2 had slightly edge over zero mapping. The following results are with u2 mapping of LBP.

A. Part 1: Without Feature Selection

In this part, we have studied the performance of the proposed method in different channels and different sub-band combinations without feature selection.

1) Effects of SPT levels on the performance within a single orientation: In this experiment, we have studied the performance of three different sub-bands. These three sub-bands are located in different levels of the SPT, but within the same orientation. All of the three sub-bands are in the first orientation. The feature vector length in this case is 256 (the number of bins in LBP histogram). Fig. 4 shows that, in all cannels, level 1 has the highest accuracy. The accuracy of the first level in Cr channel is 87.6%, which is the best of all. The accuracy of the same channel decreases to 78.6% in the second level and arrives to the third level with its lowest value of 66.8%. The same sequence, but with different values is applicable for the other channels. The ROC curves for Cr and Cb chrominance channels in Fig. 5 and Fig. 6, respectively, show how the area under the curve changed in different levels.

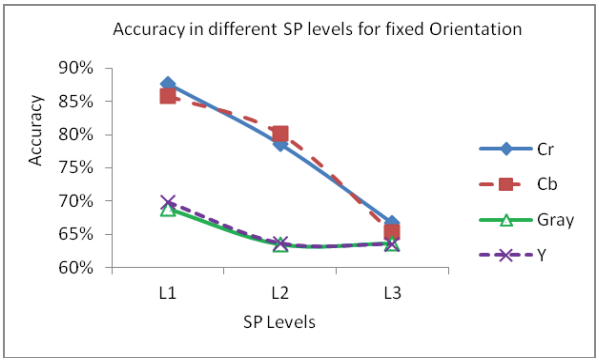

Fig. 4. Effect of different levels of SPT (Orientation 1).

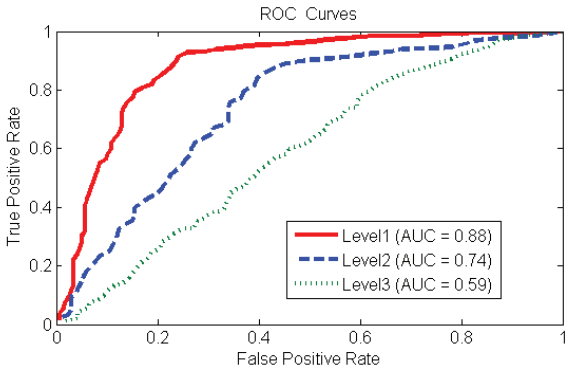

Fig. 5. ROC curves for the three levels in the first orientation for Cr channel.

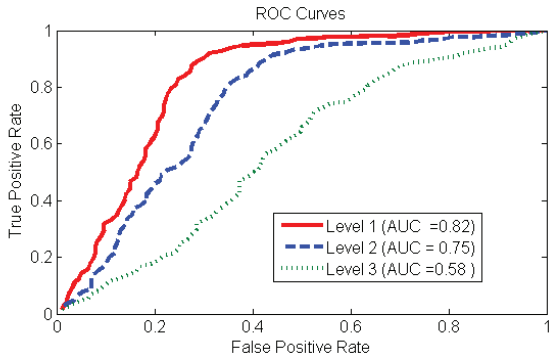

Fig. 6. ROC curves for the three levels in the first orientation for Cb channel.

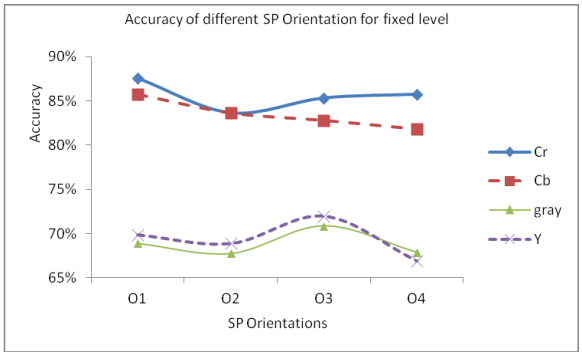

Fig. 7. Effect of different orientations of SPT (Level 1).

2) Effects of SPT orientations on the performance within a single level: In this experiment, we have studied the performance of four different sub-bands having four different orientations, but in the same level. All of the four sub-bands in this experiment are in the first level. Fig. 7 shows that, in both the chrominance channels, the first orientation has the highest accuracy, which is 87.6% for Cr and 85.8% for Cb. The second best accuracy for Cr channel (85.8%) is given by the forth orientation and the third one of value (85.4%) is given by the third orientation. The second best accuracy for Cb channel (83.7 %) is given by the second orientation and the third one of value (82.8 %) is given by the third orientation. The lowest accuracy is given for Cr by the second orientation, while it is given by the forth orientation for Cb channel. So the rank of orientations accuracy depends on the chrominance channel used. Fig. 8 and Fig. 9 show the ROC curves of the four orientations for Cr and Cb channels, respectively.

3) Effects of each SPT level on the performance: In this experiment, we have studied the effects of each complete SPT level on the performance. The histograms of the four sub-bands within each level were concatenated to form a feature vector with a length of 1024. Fig. 10 shows the accuracy of the three levels in different channels, and the ROC curves in Cr and Cb chrominance channels are shown in Fig. 11 and

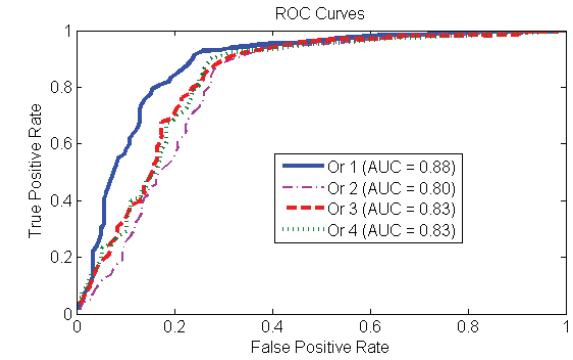

Fig. 8. ROC curves for the four orientations in the first level for Cr channel.

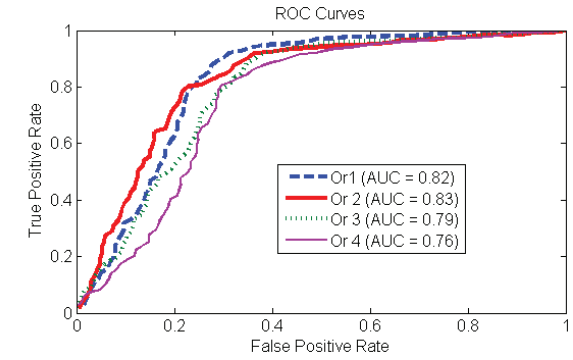

Fig. 9. ROC curves for the four orientations in the first level for Cb channel.

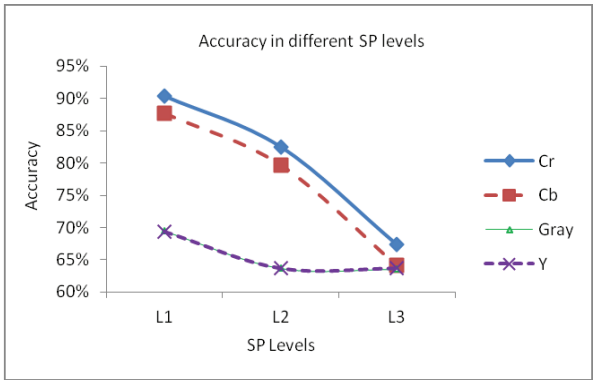

Fig. 10. Effect of different complete levels.

Fig. 12, respectively. It is clear that the main behaviour of the accuracy is very similar to that in the first experiment, even there is a good enhancement in the values. In this experiment for example, the best value for the accuracy given by the first level in Cr channel improved to 90.4% while it is only 87.6% in the first experiment. Additionally, the luminance channel (Y) and the gray scale nearly have the same accuracy in each level.

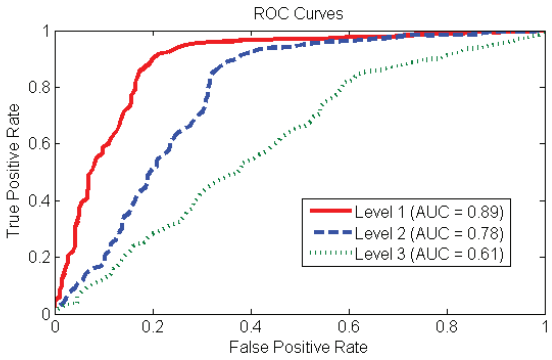

Fig. 11. ROC curves for 3 different levels of Cr channel.

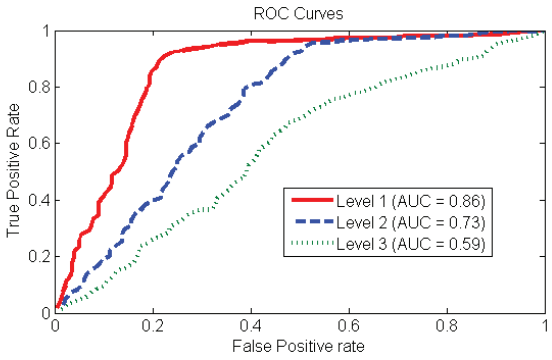

Fig. 12. ROC curves for 3 different levels of Cb channel.

4) Effects of each SPT orientation on the performance: In this experiment, we have studied the effects of each complete SPT orientation on the performance. The histograms of the three sub-bands within each orientation were concatenated to form a feature vector with a length of 768. Fig. 13 shows the accuracy of the four orientations in different channels, and Fig. 14 and Fig. 15 show the ROC curve for each orientation in both Cr and Cb channels, respectively. The main behaviour of the curves is similar to that in the second experiment, but the accuracy mainly degraded except for the third orientation. There is little bit enhancements in the accuracy of Cb and Cr components, where it goes from 85.4% to 87.3% in Cr, and from 82.8% to 86.3% for Cb. It is also noticed that the performance of different orientations is comparable within each chrominance channel. Moreover, the luminance Y and grayscale channels are performing bad comparing with Cr and Cb chrominance components.

5) Effects of combining all the sub-bands of SPT: In this experiment, we have studied the performance of combining all the sub-bands of SPT by concatenating all of the histograms. The length of feature vector in this case is 3584. Fig. 16 shows the best performance in the four different channels, which is

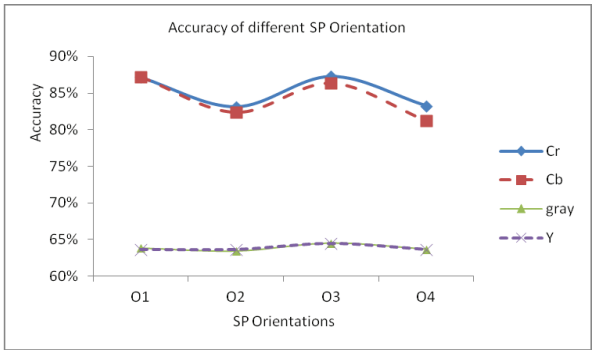

Fig. 13. Effect of different complete orientations.

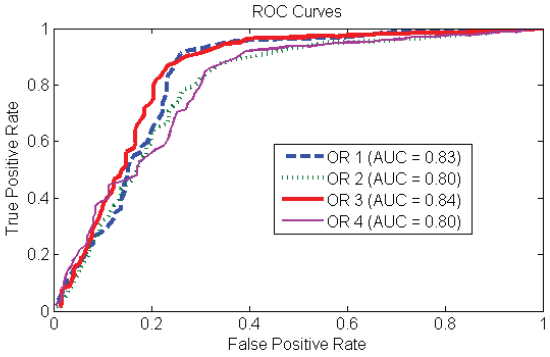

Fig. 14. ROC curves for 4 different orientations of Cr channel.

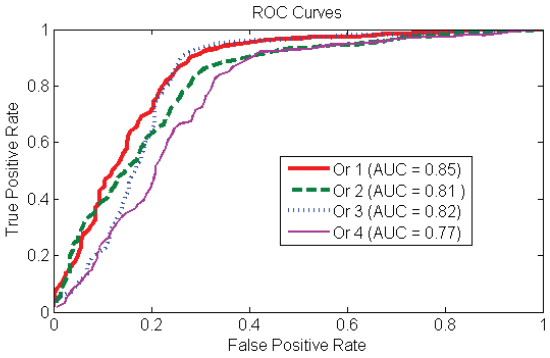

Fig. 15. ROC curves for 4 different orientations of Cb channel.

91.4% in Cr channel, 88.6% in Cb channel, 78% in Y channel, and 76.1% in grayscale. Fig. 17 show the ROC curves for each channel. It is clear that the combination of all sub-bands achieves the highest accuracy for each channel and overcome the limitations of all other combinations in the previous experiments. In addition, figures show that Cr channel provide the best accuracy followed by Cb channel, and finally, Y channel comes with comparable accuracy with the grayscale image.

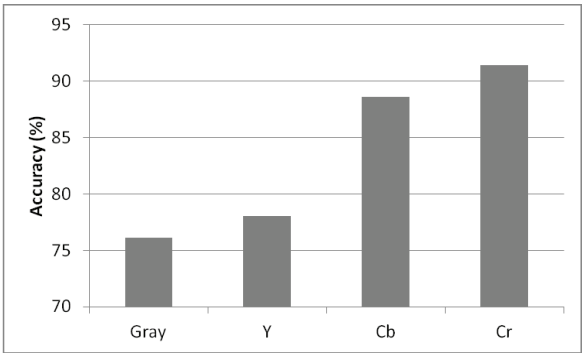

Fig. 16. The performance of combining all the sub-bands.

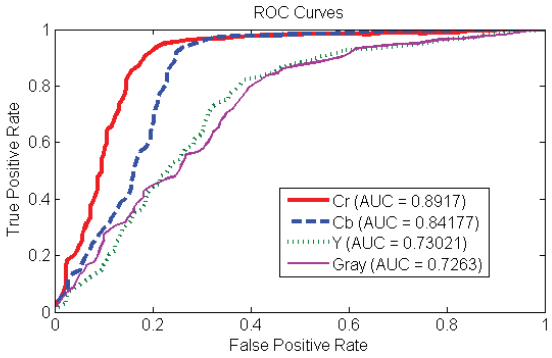

Fig. 17. ROC curves for combining all the sub-bands.

B. Part 2: With Feature Selection

In this part, the effects of feature selection on the performance have been studied. Two feature selection methods and a concatenation of them and different number of features is used each time to see how the performance of the best case from part 1 (Fig. 16) affected.

1) Testing with LOGO algorithm: Experiment 5 in the part 1 is repeated here for Cr and Cb chrominance components with the LOGO feature selection algorithm. A different number of features are selected each time and the performance is shown in Table I. By selecting 850 features out of total 3584 features, the accuracy improves from 91.4% to 92.5% in case of Cr channel, and from 88.6% to 91.8% in case of Cb channel.

2) Testing with FDR algorithm: Experiment 5 in part 1 is also repeated for Cr and Cb chrominance components with FDR selection algorithm. Table II shows the accuracy with different number of features selected. By selecting 850 features out of total 3584 features, the accuracy improves from 91.4% to 93.2% in case of Cr channel; while the best improvement was achieved in case of Cb channel using 200 features only.

3) Testing with cascading LOGO and FDR algorithms: Experiment 5 in part 1 with a cascaded feature selection of both LOGO and FDR algorithms is conducted for Cr and Cb chrominance components. The accuracy with different number selected features is in Table III.

As a result of the previous experiments, the best performance found in Cr and Cb chrominance components in case of combining all sub-bands of SPT and cascading selection for 480 features using both LOGO and FDR algorithms. Final accuracy of 95.2% was achieved with Cr channel and 93.8% with Cb channel. The details measurements of this case are shown in Table IV. AUC using each of the channels is 0.93 with a standard deviation of around 0.02 or 0.03.

TABLE 1
EFFECTS OF LOGO ALGORITHM WITH DIFFERENT NUMBER OF FEATURES ON THE ACCURACY

No of Features	50	200	480	850	1800
Acc for Cr	91.7%	90.9%	92.3%	**92.5%**	91.1%
Acc for Cb	88.5%	91.3%	90.7%	**91.8%**	90.7%

TABLE II
EFFECTS OF FDR ALGORITHM WITH DIFFERENT NUMBER OF FEATURES ON THE ACCURACY

No of Features	50	200	480	850	1800
Acc for Cr	86.6%	92.1%	91.6%	**93.2%**	90.7%
Acc for Cb	86.8%	**91.7%**	90.7%	90.3%	90.3%

TABLE III
EFFECTS OF CASCADING BOTH LOGO AND FDR ALGORITHMS WITH DIFFERENT NUMBER OF FEATURES ON THE ACCURACY

No of Features	50	200	480	850	1800
Acc for Cr	86.6%	92.7%	**95.2%**	92.8%	91.3%
Acc for Cb	89.0%	92.5%	**93.8%**	90.4%	90.0%

TABLE IV
THE BEST CASE MEASUREMENTS

	Accuracy	Sensitivity	Specificity	AUC
Cr	95.2% ± 2.2	98.7% ± 1.5	89.1% ± 6.4	0.93 ± 0.03
Cb	93.8% ± 2.5	97.9% ± 3.1	86.8%± 4.3	0.93 ± 0.02

TABLE V
COMPARISON OF PERFORMANCE BETWEEN THE PROPOSED METHODAND THE METHOD IN [14]

Image component	The proposed method	Method [14]
Cr	95.2 %	73.8 %
Cb	93.8 %	73.6 %

For comparison purpose, we choose the method described in [14] because it also uses chrominance components. In [14], the features are extracted using stationary distribution of Markov chain in a thresholded edge image. Table V shows the comparative performance of the proposed method and the method in [14]. From the table, we find that the proposed method outperforms method [14] in both the chrominance components.

From all the experiments results, we find the chrominance channels are better than luminance channel or gray scale for image forgery detection. Human eyes are sensitive to luminance channel, but forgeries are done in such a way that they are not visible in naked eyes. Therefore, the trace of the forgery might in the chrominance channels, and it is experimentally proved in this paper. The use of SPT, which is found useful in this paper, is also a new concept in the context of image forgery detection.

IV. CONCLUSION

In this paper, an improved algorithm based on SPT and LBP, to detect copy move tampering in digital images, is proposed. The image is first transformed into multiple sub-bands of different scales and orientations by SPT.

Then LBP normalized histogram extracted from each sub-band and used as a feature vector. Two feature selection methods are used to reduce dataset dimensionality. The performance was tested different combinations of sub-bands.

According to our experimental results, the combination of all sub-bands gives the best accuracy in Cr and Cb chrominance components. The accuracy for Cr and Cb channels is 95.2 % and 93.8%, respectively.

Our future work will be to localize the forgery in the images.

ACKNOWLEDGEMENT

This work is supported by the grant 10-INF1140-02 under the National Plan for Science and Technology (NPST), King Saud University, Riyadh, Saudi Arabia.

REFERENCES

[1] M. Kumar, "*Digital Image Processing*", Satellite Remote Sensing and GIS Applications in Agricultural Meteorology, pp. 81-102, July 2003.

[2] Swaminathan, A. Min Wu, Liu, K.J.R, "*Digital Image Forensics via Intrinsic Fingerprints*", IEEE Transaction on Information Forensics and Security, Vol. 3 (1), pp. 101-117, March 2008.

[3] Sunil Kumar, P. K. Das, Shally and S. Mukherjee, "*Copy-Move Forgery Detection in Digital Images: Progress and Challenges*", International Journal on Computer Science and Engineering (IJCSE), Vol. 3, pp. 652-663, Feb 2011.

[4] L. Weiqi, Q. Zhenhua, P. Feng, H. Jiwu, "*A survey of passive Technology for digital image forensics*", Frontiers of Computer Science in China, Vol. 2(1), pp. 1−11, 2007.

[5] J. Fridrich, D. Soukal, and J. Lukas, "*Detection of Copy-Move Forgery in Digital Images*", in Proceedings of Digital Forensic Research Workshop, August 2003.

[6] A.C. Popescu, H. Farid, "*Exposing Digital Forgeries by Detecting Duplicated Image Regions*", Tech. Rep, TR2004-515, Dartmouth College, 2004

[7] G. Li, Q. Wu, D. Tu, and S. Sun, "*A Sorted Neighborhood Approach For Detecting Duplicated Regions in Image Forgeries based on DWT and SVD*", in Proceedings of IEEE International Conference on Multimedia and Expo, Beijing China, pp. 1750-1753, July 2-5, 2007.

[8] S. Bayram, H. T. Sencar, N. Memon, "*An efficient and robust method for detecting copy-move forgery*", Proc. ICASSP09, pp. 1053-1056, 2009.

[9] Y. Huang, W. Lu, W. Sun, D. Long, "*Improved DCT-based detection of copy-move forgery in images*", Forensic Science International, Vol. 206, Issues 1-3, pp. 178-184, March 2011.

[10] G. Muhammad, M. Hussain, and G. Bebis, "*Passive copy move image forgery detection using undecimated dyadic wavelet transform*," Digital Investigation, Vol. 9, Issue 1, pp. 49-57, 2012.

[11] M. Unser, N. Chenouard, V. D. Ville D, " *Steerable Pyramids and Tight Wavelet frames in L2 (Rd)*", IEEE transactions on image processing, Vol.20, No. 10, pp. 2705-2721, Oct, 2011.

[12] T. Ahonen, A. Hadid, and M. Pietikainen, " *Face Description with Local Binary Patterns: Application to Face Recognition*", IEEE Transactions on Pattern Analysis and Machine Intelligence, Vol. 28, No. 12, December 2006.

[13] CASIA image tampering detection evaluation database (CASIA TIDE) V1.0, available at http://forensics.idealtest.org.

[14] W. Wang, J. Dong, and T. Tan, "*Image tampering detection based on stationary distribution of Markov chain*", in 17th IEEE International Conference on Image Processing (ICIP), pp.2101 –2104, 2010.

[15] Y. Sun, S. Todorovic, and S. Goodison," *Local Learning Based Feature Selection for High Dimensional Data Analysis*", IEEE Trans. on Pattern Analysis and Machine Intelligence, vol. 32, no. 9, pp. 1610-1626, 2010